Process intensification of synthesis of metal organic framework particles assisted by ultrasound irradiation

Ogura, Yu ; Taniya, Keita ; Horie, Takafumi ; Tung, Kuo-Lun ; Nishiyama, Satoru ; Komoda, Yoshiyuki ; Ohmura, Naoto

(Citation)
Ultrasonics Sonochemistry,96:106443

(Issue Date)
2023-06

(Resource Type)
journal article

(Version)
Version of Record

Ultrasonics Sonochemistry 96 (2023) 106443

Contents lists available at ScienceDirect

Ultrasonics Sonochemistry

journal homepage: www.elsevier.com/locate/ultson

Process intensification of synthesis of metal organic framework particles assisted by ultrasound irradiation

Yu Ogura [a], Keita Taniya [a], Takafumi Horie [b], Kuo-Lun Tung [c], Satoru Nishiyama [a], Yoshiyuki Komoda [a], Naoto Ohmura [a,*]

[a] Department of Chemical Science and Engineering, Graduate School of Engineering, Kobe University, Japan
[b] Department of Chemical Engineering, Graduate School of Engineering, Osaka Metropolitan University, Japan
[c] Department of Chemical Engineering, National Taiwan University, Taiwan

ARTICLE INFO

Keywords:
Zr-MOF
UiO-66
Ultrasound-assisted synthesis method
Process intensification

ABSTRACT

This study synthesized UiO-66, a typical Zr-Metal Organic Framework (MOF), by using an ultrasound-assisted synthesis method to reduce the synthesis time. This method was short-time ultrasound irradiation at the initial stage of the reaction. As compared with average particle size of conventional solvothermal method (=192 nm), averaged particle size by the ultrasound-assisted synthesis method showed particle sizes that were smaller on average, ranging from 56 to 155 nm. In order to compare the relative reaction rates of the solvothermal method and the ultrasound-assisted synthesis method, the cloudiness of the reaction solution in the reactor was observed with a video camera, and the luminance was calculated from the images obtained by the video camera. It was found that the ultrasound-assisted synthesis method showed a faster increase in luminance and shorter induction time than the solvothermal method. The slope of the luminance increase during the transient period was also found to become increase with the addition of ultrasound, which also affects the growth of particles. Observation of the aliquoted reaction solution confirmed that particle growth was faster in the ultrasound-assisted synthesis method than in the solvothermal method. Numerical simulations were also performed using MATLAB ver. 5.5 to analyze the unique reaction field generated by ultrasound. Bubble radius and temperature inside a cavitation bubble was obtained using the Keller-Miksis equation, which reproduces the motion of a single bubble. The bubble radius expanded and contracted repeatedly according to the ultrasound sound pressure, and eventually collapsed. The temperature at the time of collapse was extremely high, exceeding 17,000 K. It was confirmed that the high-temperature reaction field generated by ultrasound irradiation promoted nucleation, leading to a reduction in particle size and induction time.

1. Introduction

Metal organic frameworks (MOFs) are a type of crystalline polymer complexes formed by organic ligands bridging metal ions, and are materials with a porous coordination network structure with a high surface area far exceeding that of activated carbon and zeolites. In addition to metal ions and organic ligands, solvents and crystal growth regulators are used in the synthesis of MOFs [1]. The metal ions and organic ligands are important factors in determining the pore size and properties of MOFs, which can impart magnetic, conductive, and dielectric properties. Most MOFs are prepared in pure N,N-diethylformamide (DEF) or N, N-dimethylformamide (DMF) solvents, which decompose at high temperatures to form amine bases that slowly deprotonate the organic functional groups of the organic ligands to form coordination bonds by the combination of a metal ion and an organic ligand to form MOFs. Since the coordination bond is an equilibrium reaction between the metal ion and the organic ligand, a crystal control agent is used to control the reach rate and direction of an equilibrium state. During crystal growth, bridging ligands and metal ions continue to alternately form coordination bonds on the surface of the generated crystal nuclei. A crystal control agent such as acetic acid can be added simultaneously with metal ions and organic ligands to block the outer surface of the MOF crystals to some extent and control crystal size.

During in MOF synthesis, the temperature at which the reaction takes place is another important factor. Since sufficient activation energy for the reaction cannot be obtained at room temperature, heating

* Corresponding author at: 1-1 Rokko-dai, Nada-ku, Kobe 657-8501, Japan(Naoto Ohmura).
E-mail address: ohmura@kobe-u.ac.jp (N. Ohmura).

https://doi.org/10.1016/j.ultsonch.2023.106443
Received 27 February 2023; Received in revised form 25 April 2023; Accepted 14 May 2023
Available online 18 May 2023

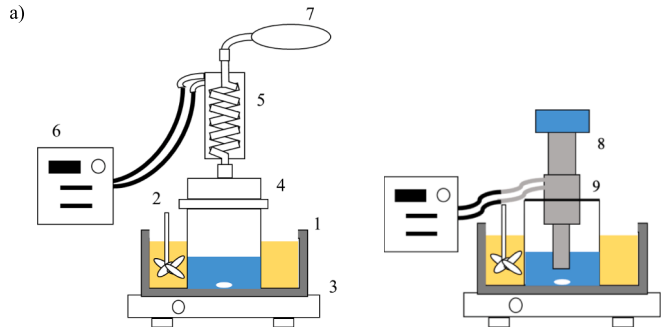

Fig. 1. Experimental set-up: 1. Stainless bucket, 2. Stirring bar, 3. Hot magnetic stirrer, 4. Separable flask, 5. Reflux condenser, 6. Chiller and 7. Balloon (for sealing).

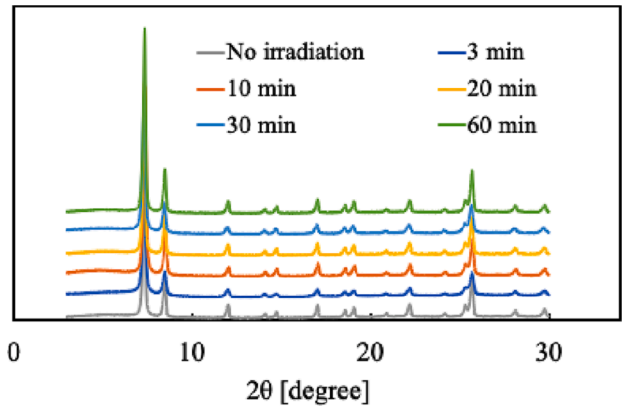

Fig. 4. XRD patterns of UiO-66.

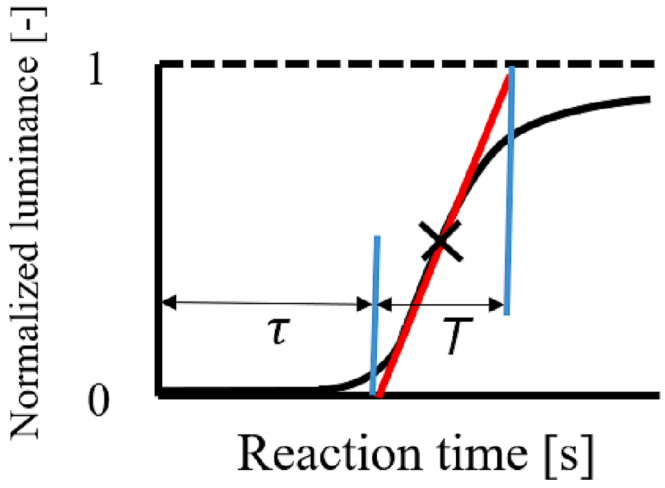

Fig. 2. Schematic of time variation of luminance.

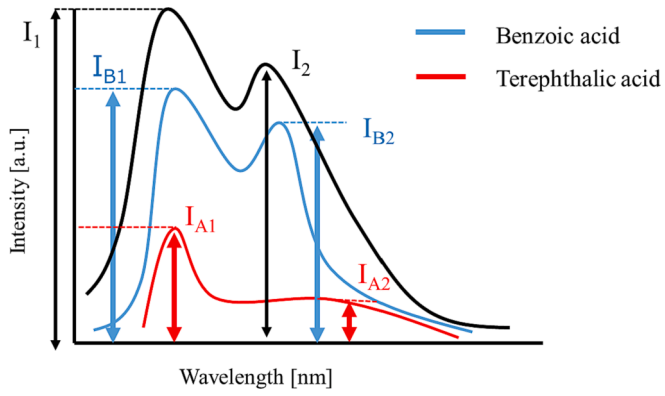

Fig. 3. Spectrophotometer model diagram.

Table 1
Symbols and their values used in numerical simulation.

S	Surface tension [N/m]	0.036
ρ_L	Density [kg/m^3]	944
μ_L	Viscosity [Pa s]	0.0008
c	Sound velocity [m/s]	1500
P_v	Vapor pressure [Pa]	4930
f	Ultrasound frequency [kHz]	20
P_{stat}	Static pressure [Pa]	101,325
R_0	Initial radius of the bubble [μm]	5

methods are used to synthesize MOFs. Depending on the temperature range, the heating methods can be roughly classified into two kinds: the reflux method, in which the solvent is heated below the boiling point at ambient pressure, and the solvothermal methods, in which the solvent is heated above the boiling point in a pressure-resistant sealed vessel under high temperature and high pressure. In the solvothermal methods, when water is used as a solvent, it is known as hydrothermal synthesis [2]. Although solvents under high temperature and high pressure improve solubility and increase the reaction rate to synthesize MOF, still the long reaction time is required. Other synthesis methods which drastically reduce reaction time have been, therefore, explored.

From the aspect of process intensification, utilizing ultrasonic irradiation is one of the potential methods to produce nanomaterials. For example, Nagatomo et al. [3] used ultrasonic irradiation for pretreatment of emulsion polymerization of styrene. They successfully showed that the pretreatment of ultrasonic irradiation as short as 1 min drastically improved monomer dispersion and increased reaction rate even under the agitation condition with low rotational speed of impeller. Recently, ultrasound-assisted synthesis has also been widely used for MOF synthesis [4]. The ultrasound-assisted synthesis method involves the addition of ultrasound irradiation to the usual high-temperature heating or solvothermal method. Ultrasonic irradiation produces a localized high temperature and pressure field due to the collapse of cavitation bubbles, resulting in accelerated reactions and shorter reaction times [5]. As the high-temperature field is localized, the reaction can be safely performed under moderate temperature conditions. Additionally, liquid flow directed toward the center of the bubble during bubble contraction is recoiled during collapse, creating shock waves and microjets toward the bubble's periphery, which effectively agitate and mix the liquid [6]. Since Qiu et al. [7] first succeeded in synthesizing MOFs using ultrasound in 2008, many studies have been conducted on MOF synthesis using ultrasound. Ultrasound irradiation not only shortens the reaction time and allows for milder conditions, but also influences the shape of the particles. Although the behavior varies depending on the MOF being synthesized, it has been reported that the particle size of MOFs synthesized using ultrasound can be controlled by varying the temperature and ultrasound output, as compared to MOFs synthesized using conventional heating methods [8,9].

This study reports on UiO-66 (UiO: Universitet i Oslo = University of Oslo), a representative among Zr-based metal–organic frameworks (Zr-MOFs) that use Zr as the metal ion. UiO-66 was synthesized using zirconium ion (Zr^{4+}) as a metal ion and highly hydrophobic terephthalic acid as an organic ligand to form a highly water-resistant structure [10]. UiO-66 has also been used as a catalyst for the decomposition of toxic gases in reactions other than those involving water. In this case, it was found that the reaction rate largely depends on particle size. It is, therefore, necessary to control the particle size of UiO-66. However, the effect of ultrasound irradiation on the particle size of UiO-66 has not

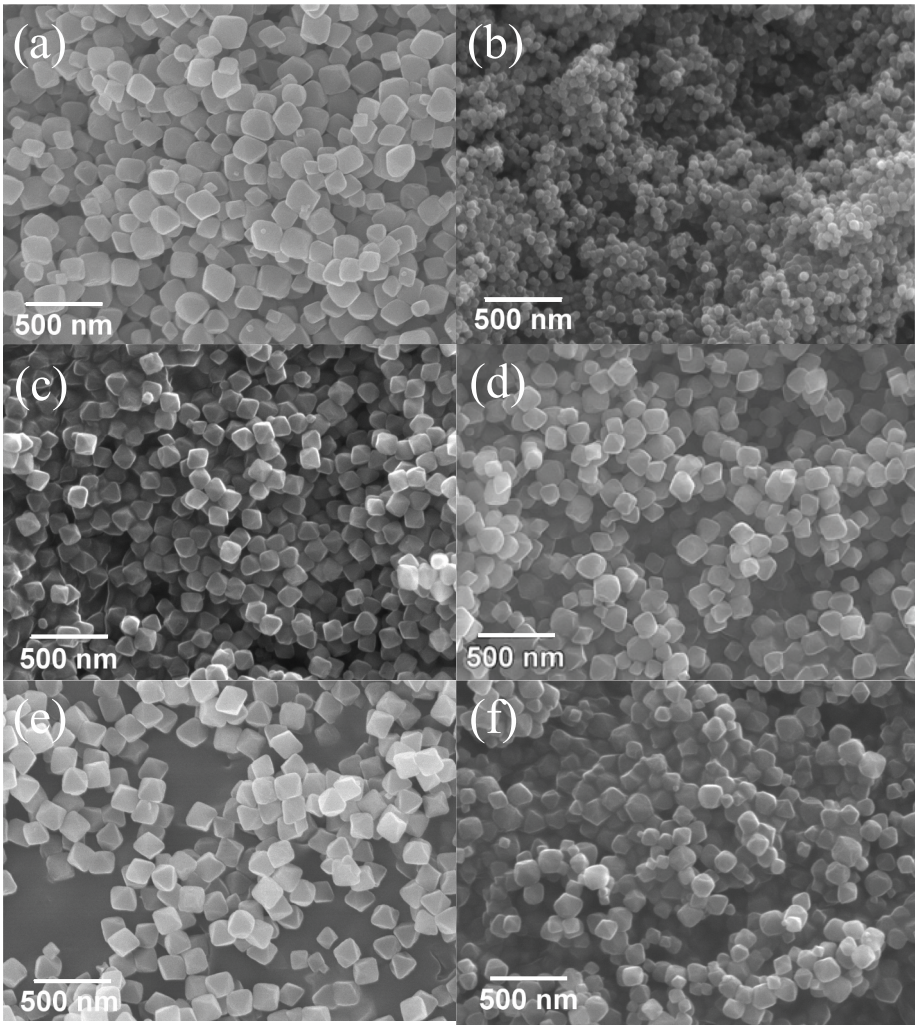

Fig. 5. SEM images of (a) UiO-66 without ultrasound irradiation and (b) 3 min ultrasound irradiation (c) 10 min (d) 20 min (e) 30 min (f) 60 min.

been clarified. In crystallization, nuclei are generated by increasing supersaturation, and the structure is formed by the growth of the nuclei. Since the initial stage of the reaction during nucleation contributes significantly to the particle size, studies have been conducted to observe the particle size by ultrasound irradiation during the initial stage of the reaction when nuclei are produced [11]. This study, therefore, investigated the effect of ultrasound irradiation on the particle size of UiO-66 and the reaction process by irradiating UiO-66 in the early stage of the reaction.

2. Materials and methods

The synthesis of UiO-66 was prepared based on the method of Schaate et al. [12]. The reaction solution consisted of 2.6 mmol of zirconium chloride (Wako Pure Chemical Industries) as a Zr precursor, 77.4 mmol of benzoic acid (Wako Pure Chemical Industries) as a crystal growth regulator, and 150 mL of N,N-dimethylformamide (DMF) (Wako Pure Chemical Industries) as a solvent. The mixture of the above reagents was heated to 393 K in a separable flask made of glass with 500 mL capacity and a transparent reaction solution was obtained. 3.8 mmol of powdered terephthalic acid (Wako Pure Chemical Industries) as the organic ligand was added to the aforementioned separable flask, and the synthesis was carried out at 393 K for 24 h using the apparatus shown in Fig. 1. At the beginning of the synthesis, ultrasound irradiation was performed using a horn-type ultrasound irradiator (US-300 T, Nippon Seiki) at 393 K and 20 kHz frequency. The reactor is immersed in an oil bath, and both the oil bath and the inside of the reactor are stirred, so the heat transfer performance is relatively high, and the temperature was maintained at 393 K even during ultrasonic irradiation. Ultrasound energy passing through the liquid is partially converted into thermal energy. Since there is a proportional relationship between the initial temperature increase in the solution and the ultrasound energy [15], the ultrasound power P_U was calculated by Eq. (1) using the calorimetry method [16],

$$P_U = MC_P\frac{\Delta T}{\Delta t} \quad (1)$$

where M [kg] is the mass of the sample suspension, C_p [J・kg^{-1}・K^{-1}] is the specific heat of the sample suspension, and $\Delta T/\Delta t$ is the rate of temperature increase of the sample suspension. The temperature change was measured when 150 g of distilled water was irradiated with ultrasound. From the calorimetric calculations, $P_U = 41$ W was obtained. The ultrasound irradiator horn tip was fixed at a position where it was immersed in the liquid by 30 mm, and the flask was covered with aluminum foil to prevent leakage of gas in the flask. The ultrasound irradiation time was varied at 3, 10, 20, 30, 60 min. About 30 min after heating, white crystals precipitated from the reaction solution and were suspended. The suspension was centrifuged at 3500 rpm for 10 min to obtain a white powder. The powder was immersed in 50 mL of DMF or methanol, sonicated for 10 min, centrifuged at 3500 rpm for 10 min, and washed by discarding the supernatant liquid. This washing process was performed three times with DMF and with methanol, respectively. After

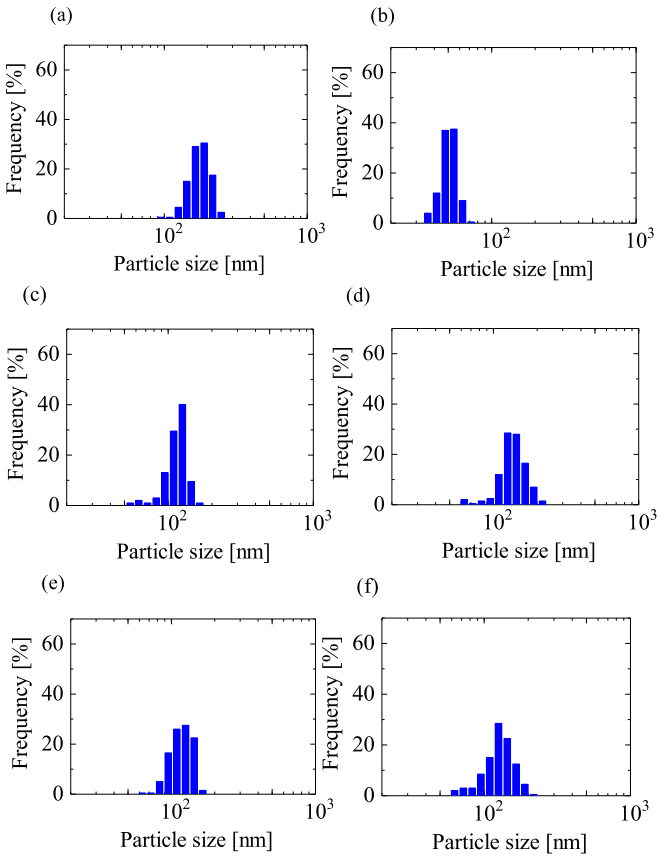

Fig. 6. The particle size distribution of (a) UiO-66 without ultrasound irradiation and (b) 3 min ultrasound irradiation (c) 10 min (d) 20 min (e) 30 min (f) 60 min.

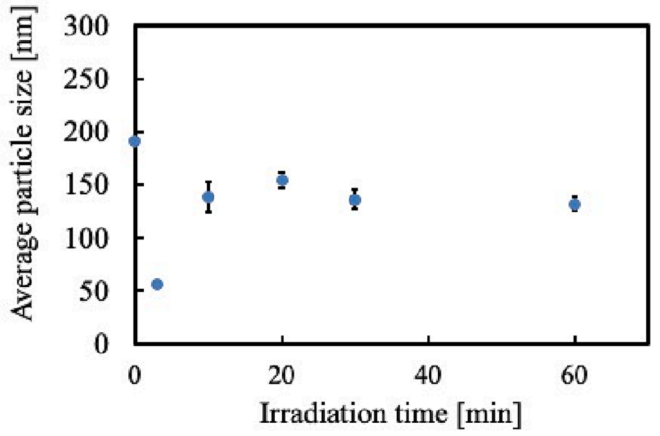

Fig. 7. Dependency of irradiation time on crystal size.

washing, the white powder was dried at 393 K for 24 h to evaporate the solvent remaining in the pores to obtain pure crystals of UiO-66.

To investigate the crystal structure of the synthesized UiO-66, X-ray diffraction measurements (RIGAKU ELECTRIC X-ray diffractometer RINT 2100) were performed at room temperature. To measure the particle size of the synthesized UiO-66, the morphology of the UiO-66 particles was observed using a scanning electron microscope (JEOL Field Emission Scanning Electron Microscope (FE-SEM) JSM-7100F. Osmium deposition was performed at a pressure of 8 Pa for 15 s before the measurement. The particle weight per particle was calculated from the measured average particle size, and the number of particles was

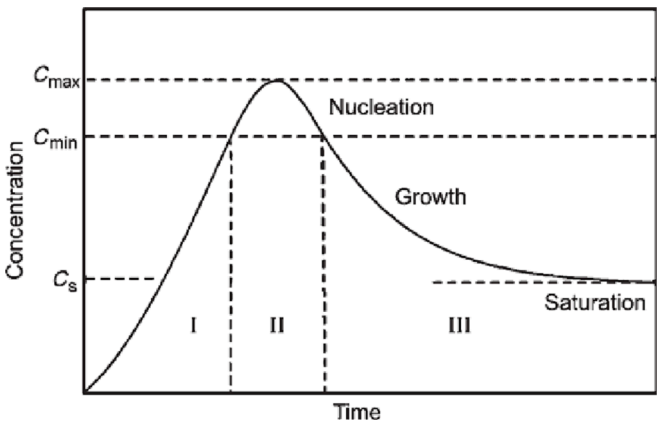

Fig. 8. LaMer model used to describe nucleation and nucleus growth.

Table 2
Number of particles of UiO-66.

Irradiation time [min]	No irradiation	3	10	20	30	60
Number of particles [$\times 10^{14}$]	4.91	184	12.7	10.2	13.3	14.2

Table 3
Particle size and coefficient of variation of UiO-66.

Irradiation time [min]	No irradiation	3	10	20	30	60
Average particle size [nm]	192	56	139	148	136	132
CV [–]	0.22	0.13	0.14	0.20	0.18	0.24

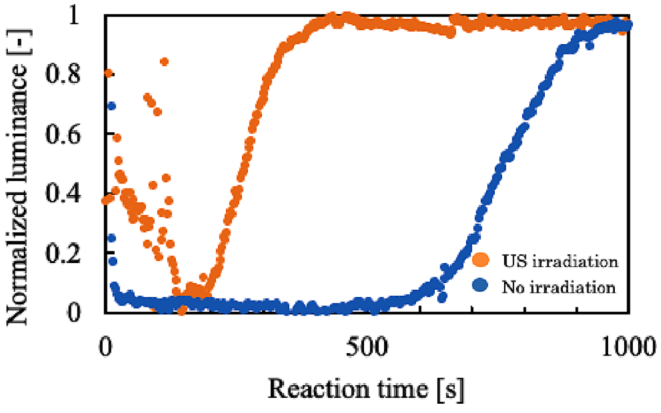

Fig. 9. Time variation of normalized luminance.

Table 4
Comparison of induction time, τ, and transient time, *T*.

US irradiation	τ [s]	*T* [s]
○	228	68
×	668	122

calculated by Eq. (2) using the dry weight and particle weight.

$$\text{Number of particles}\,[\%] = \frac{\text{Sample weight after drying}[g]}{\text{Weight per particles}[g]} \quad (2)$$

As the UiO-66 synthesis proceeds, the transparent reaction solution

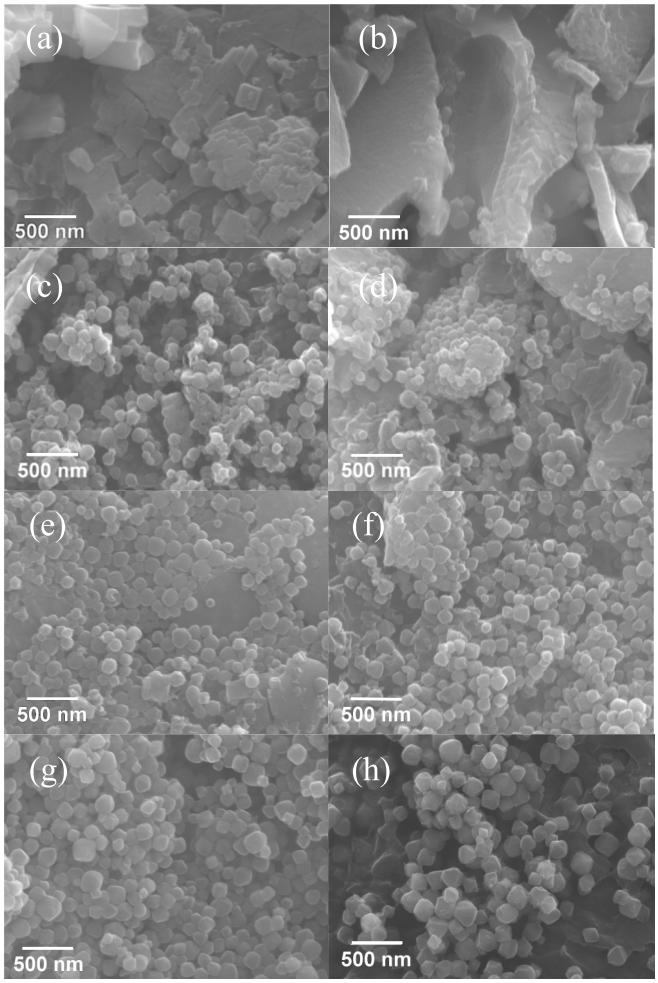

Fig. 10. UiO-66 particle growth SEM images without ultrasound irradiation in reaction time of (a) 0 min (b) 3 min (c) 7 min (d) 10 min (e) 20 min (f) 30 min (g) 60 min (h) 90 min.

becomes opaque due to the precipitation of white crystals. This phenomenon was captured with a digital video camera (Panasonic HC-WXF1M, frame rate 20 fps, 480 × 272 pixels, aspect ratio 1,image scale: 0.275 mm/pixel), and the process of cloudiness of the reaction solution was analyzed with the image analysis software Image J software. Luminance of image is an indicator of brightness and increases as the cloudiness progresses. A time variation of the luminance increase can be approximated with a delay system with induction time. Fig. 2 shows a schematic diagram of the graph. Since the reaction is transparent at the beginning, the luminance value is 0, and the induction time τ is calculated as the time from which the luminance begins to increase. The time when the reaction progresses from clear and colorless to cloudy liquid was calculated as the transient period.

The structure of UiO-66 is a three-dimensional network structure consisting of alternating coordination bonds between the metal ion zirconium ion (Zr^{4+}) and the organic ligand terephthalic acid precipitated as white solid powders. The reaction solution can be separated into solid UiO-66 and unreacted sample by centrifugation. The supernatant liquid, which is the unreacted sample, was measured spectrophotometrically (JASCO V-650). Fig. 3 shows a schematic diagram of the spectrophotometer data. The Eqs. (3)–(6) were used with the unreacted percentage of terephthalic acid as α and the unreacted percentage of benzoic acid as β. I_1 and I_2 are the peaks of the aliquots;

$$I_1 = \alpha I_{A1} + \beta I_{B1} \tag{3}$$

$$I_2 = \alpha I_{A2} + \beta I_{B2} \tag{4}$$

$$\alpha = \frac{I_1 I_{B2} - I_2 I_{B1}}{I_{A1} I_{B2} - I_{A2} I_{B1}} \tag{5}$$

$$\beta = \frac{I_1 I_{A2} - I_2 I_{A1}}{I_{B1} I_{A2} - I_{B2} I_{A1}} \tag{7}$$

where the sets of I_{A1} and I_{A2}, and I_{B1} and I_{B2} are the two peaks measured for terephthalic acid and benzoic acid alone, respectively. I_{A1} and I_{B1} measured peaks at a wavelength of 265 nm, and I_{A2} and I_{B2} measured peaks at a wavelength of 280 nm.

3. Numerical simulation of bubble dynamics

MATLAB® (Math Works Co., Ltd.) was used to calculate the pressure P applied to the bubble wall and the bubble expansion rate R/R_0 over time from the Keller-Miksis equation [12]. The equation used in this study is as follows;

$$\left(1 - \frac{\dot{R}}{C}\right) R\ddot{R} + \frac{3}{2}\dot{R}^2\left(1 - \frac{\dot{R}}{3C}\right) = \left(1 - \frac{\dot{R}}{C}\right)\frac{P}{\rho_L} + \frac{R}{\rho_L}\dot{P} \tag{7}$$

$$P = \left(p_{stat} - p_V(T_\infty) + \frac{2S}{R_0}\right)\left(\frac{R_0}{R}\right)^{3k} - \frac{2S}{R} - \frac{4\mu_L \dot{R}}{R} - p_{stat} + p_V(T_\infty) - A\sin(2\pi f t) \tag{8}$$

Symbols and their values of all parameters used in the bubble dynamics calculations are listed in Table 1. All properties except sound speed in Table 1 were taken from the Chemical Engineering Handbook (Society of Chemical Engineers, Japan) [13], and the sound speed in DMF was taken as an approximate value of 1500 m/s based on Attri *et al.* [14]. Note that the above equation assumes that the bubble is isolated, does not interact with surrounding bubbles, and oscillates spherically and symmetrically. The temperature inside the bubble was calculated using the bubble radius calculated in Eq. (7). The temperature inside the bubble was calculated using the following equation.

$$T = T_\infty \left(\frac{R_{max}}{R}\right)^{3(\gamma-1)} \tag{9}$$

4. Results and discussion

4.1. XRD measurement results

To confirm the crystal structure of the prepared Zr-MOFs, powder X-ray diffraction was measured. Fig. 4 shows the XRD patterns of UiO-66 under each ultrasound irradiation condition. The XRD patterns of UiO-66 obtained without ultrasound irradiation consists of peaks at 7.3°, 8.6°, 12.0°, 14.1°, 14.8°, 17.0°, 18.6°, 19.1°, 21.9°, 22.2°, 24.2°, 25.3°, 25.7°, 28.2° and 29.8°. These peaks correspond to the previous work [17]. The same peaks are also found in the XRD patterns obtained by ultrasonic irradiation. Therefore, the crystal structure of UiO-66 obtained by ultrasound irradiation was confirmed to be the same as that of MOF obtained without ultrasound irradiation.

4.2. Morphological observation and particle size measurement

The morphology of UiO-66 was observed using a scanning electron microscope. Fig. 5 shows UiO-66 SEM images under each irradiation condition. The characteristic octahedral crystal morphology of UiO-66, as reported previously [12], was observed in all Zr-based metal–organic frameworks. The longest part of particle was selected as the representative particle diameter, and the particle diameters of 200 particles were each measured using 40,000 × SEM images, from which the number-average particle diameter was calculated. Fig. 6 shows the particle

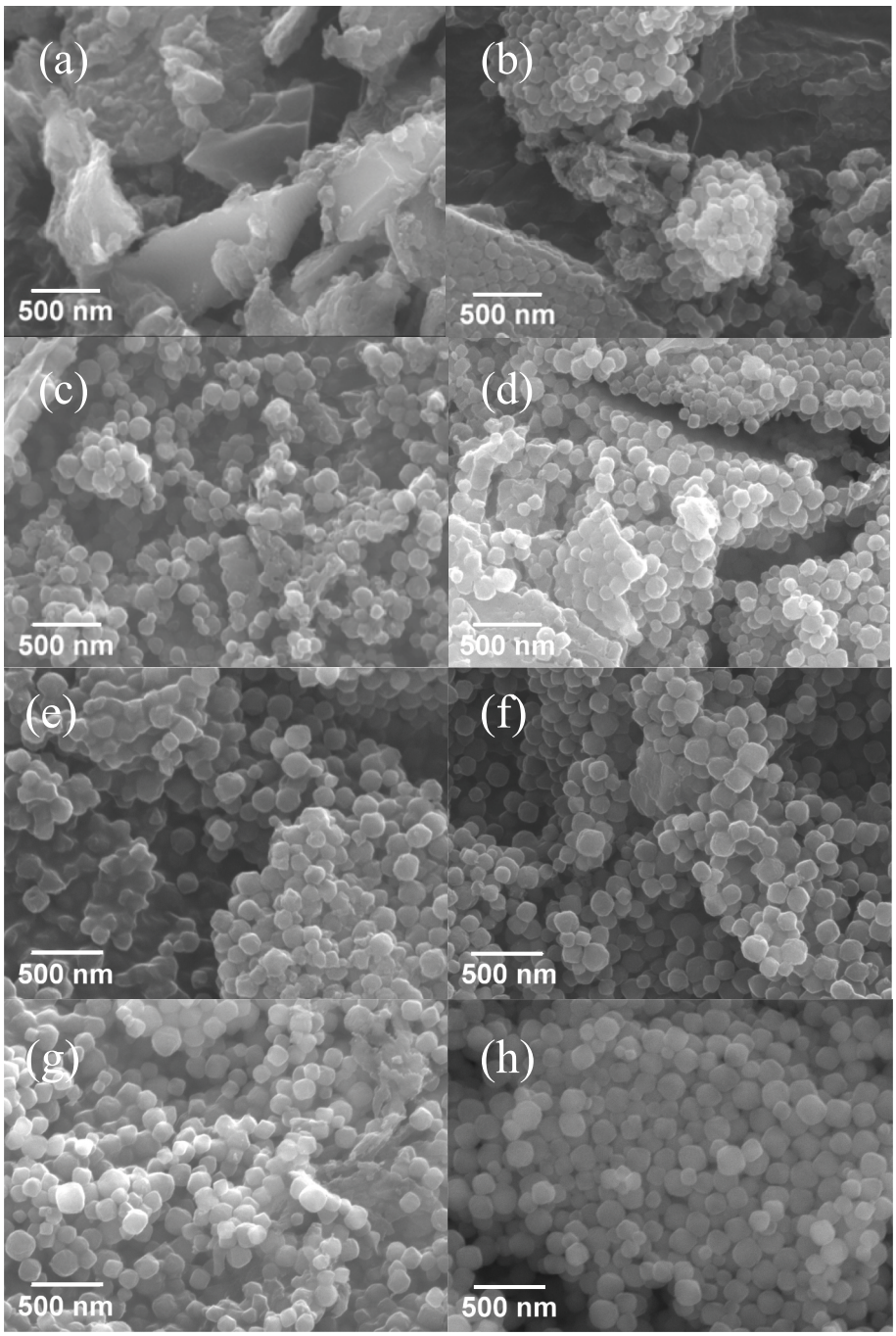

Fig. 11. UiO-66 particle growth SEM images with ultrasound irradiation in reaction time of (a) 0 min (b) 3 min (c) 7 min (d) 10 min (e) 20 min (f) 30 min (g) 60 min (h) 90 min.

size distributions of UiO-66 at each irradiation time based on this particle size measurement. Every distribution has a unimodal peak. Fig. 7 shows the relationship between irradiation time and average particle size of UiO-66. The average particle diameter was the smallest at irradiation time of 3 min, and no significant change in particle diameter can be observed at irradiation time longer than 10 min. Fig. 8 shows the LaMer Model, a particle generation model, to explain the mechanism behind particle formation [18]. The model plots solute concentration versus time and divides the particle formation process into three stages based on the solute concentration. Initially, the solution is unsaturated and exists in a stable region where no nucleation occurs. As the reaction proceeds, the solution moves into a metastable region where it is supersaturated but still no nucleation occurs. Finally, at a certain critical supersaturation concentration C_{min}, the reaction's energy exceeds the activation energy for nucleation, and the solution enters an unstable region where nucleation occurs. The high-temperature and high-pressure state due to cavitation generated by ultrasonic irradiation can induce nucleation. The metastable region becomes narrower, and the critical saturation concentration C_{min}, which is the boundary between the metastable region and the unstable region, decreases. This leads to more nucleation compared to the absence of ultrasound irradiation [19]. The increase in the number of nuclei is assumed to have resulted in a decrease in particle size because less solute is used for crystal growth per nucleus. Table 2 shows the number of particles at each irradiation time. It can be seen that the number of particles is larger with ultrasound irradiation compared to without irradiation. This indicates that

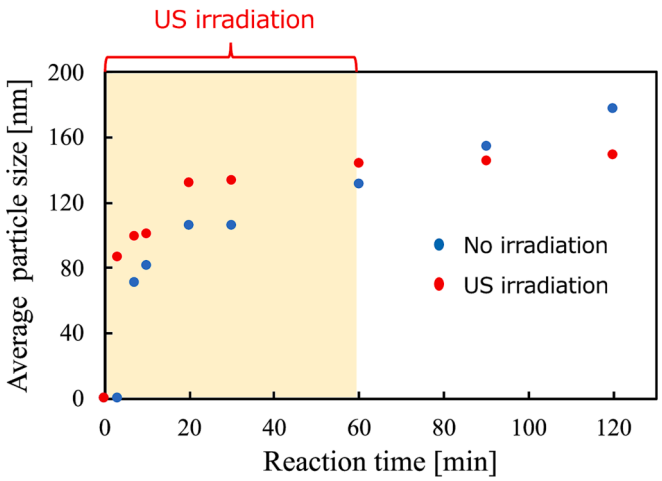

Fig. 12. Time variation of average particle size of UiO-66.

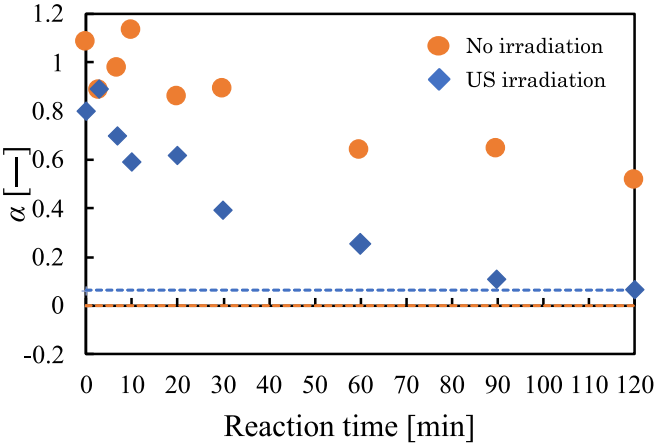

Fig. 13. Time variation of terephthalic acid unreacted ratio.

ultrasound irradiation increased the number of nuclei. When UiO-66 particles are used as catalysts, the smaller particle size is industrially advantageous because it leads to a higher catalyst packing ratio. However, with increasing the irradiation time from 3 min, the average particle size increased. This is thought to be due to Ostwald growth, a process in which small particles dissolve and contribute to the growth of larger particles. Salinas et al. [20] revealed that the high temperature and pressure conditions generated by ultrasound irradiation promote the dissolution of small particles, which may have contributed to Ostwald growth in this study.

The coefficient of variation (CV), which is based on the mean particle size, was used as a measure of particle variability. Table 3 displays the average particle size and CV obtained from SEM images at each irradiation time. Comparing the samples obtained without ultrasound irradiation to those with ultrasound irradiation, the CV values decreased, except for the irradiation time of 60 min. This decrease in variability is because the solvothermal method without ultrasound irradiation causes gradual nucleation, which results in variations in particle size. However, ultrasound waves generate a high-temperature and high-pressure state due to cavitation, which makes nucleation easier. Since nucleation occurs simultaneously with the ultrasound irradiation, it is thought that the variation in particle size is reduced.

4.3. Effect of ultrasound irradiation on induction time and transients

To observe the reaction of UiO-66, a digital video camera was used to take pictures of the inside of the reactor. Fig. 9 shows the relationship between reaction time and the dimensionless luminance value normalized by the maximum luminance value. Because terephthalic acid was fed in first, the solution inevitably became cloudy until the white powder was fully dissolved, and in the initial stage of the ultrasonic irradiation condition, bubbles caused by ultrasonic waves were generated. Therefore, the luminance was unstable at the beginning and decreased as the terephthalic acid dissolved. By using an identification method of dead time in process system engineering, a tangent line was drawn from the inflection point of the graph, and the time when the tangent line intersected the time axis was defined as the induction time τ, and the difference between the time when the tangent line intersected the steady state line and the transient period was defined as T. Table 4 shows the induction time, τ, and transient period, T. The induction time without ultrasound irradiation was $\tau = 11$ min, while the induction time with ultrasound irradiation was $\tau = 4$ min. The induction time was reduced by one-third due to the enhancement of nucleation by ultrasound irradiation. During the transient period, the time reaching the dimensionless luminance value from 0 to 1 was $T = 2$ min without ultrasound irradiation while $T = 1$ min with ultrasound irradiation. In the absence of ultrasound irradiation, heterogeneous nucleation occurs due to supersaturation. Under conditions with ultrasound irradiation, in addition to heterogeneous nucleation, nucleation due to collapse of the cavitation bubbles results in a shorter induction time. The shortened transient period is thought to be due to the fact that ultrasound irradiation caused active nucleation, which also accelerated the white turbidity.

4.4. Effect of ultrasound irradiation on nucleation and particle growth

Figs. 10 and 11 show UiO-66 SEM images for each reaction time synthesized by the solvothermal method and the ultrasound-assisted synthesis method, respectively. In the case without ultrasound irradiation, particles were visible in the SEM image at the reaction time of 7 min. In the case with ultrasound irradiation, particles were visible in the SEM image at a reaction time of 3 min. In both conditions, particle growth was observed as the reaction progressed. As shown in Fig. 12, in the case without ultrasound irradiation, the particles grew slowly as the reaction proceeded. On the other hand, in the case of ultrasound irradiation, particle growth could hardly be observed after 60 min, when

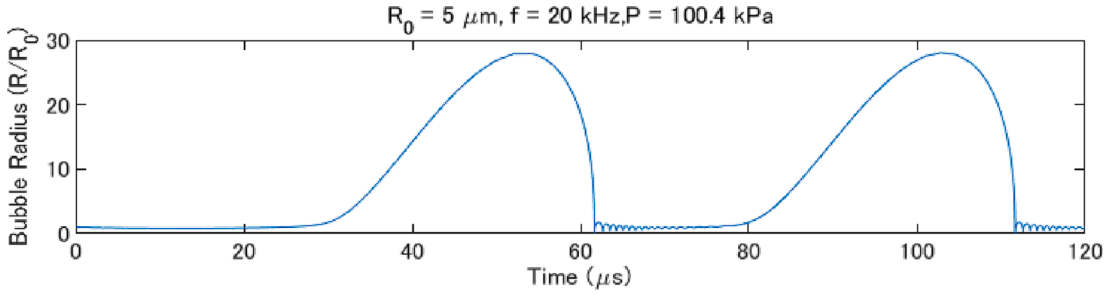

Fig. 14. Time variation of bubble radius ratio (R/R_0).

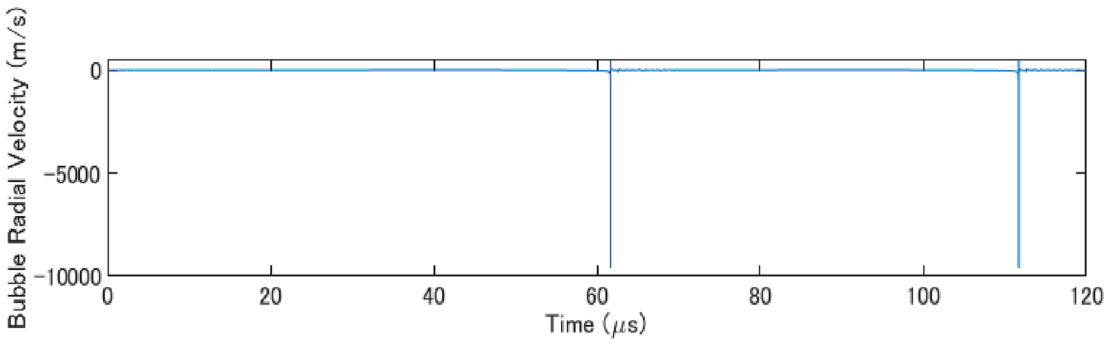

Fig. 15. Time variation of bubble radical velocity.

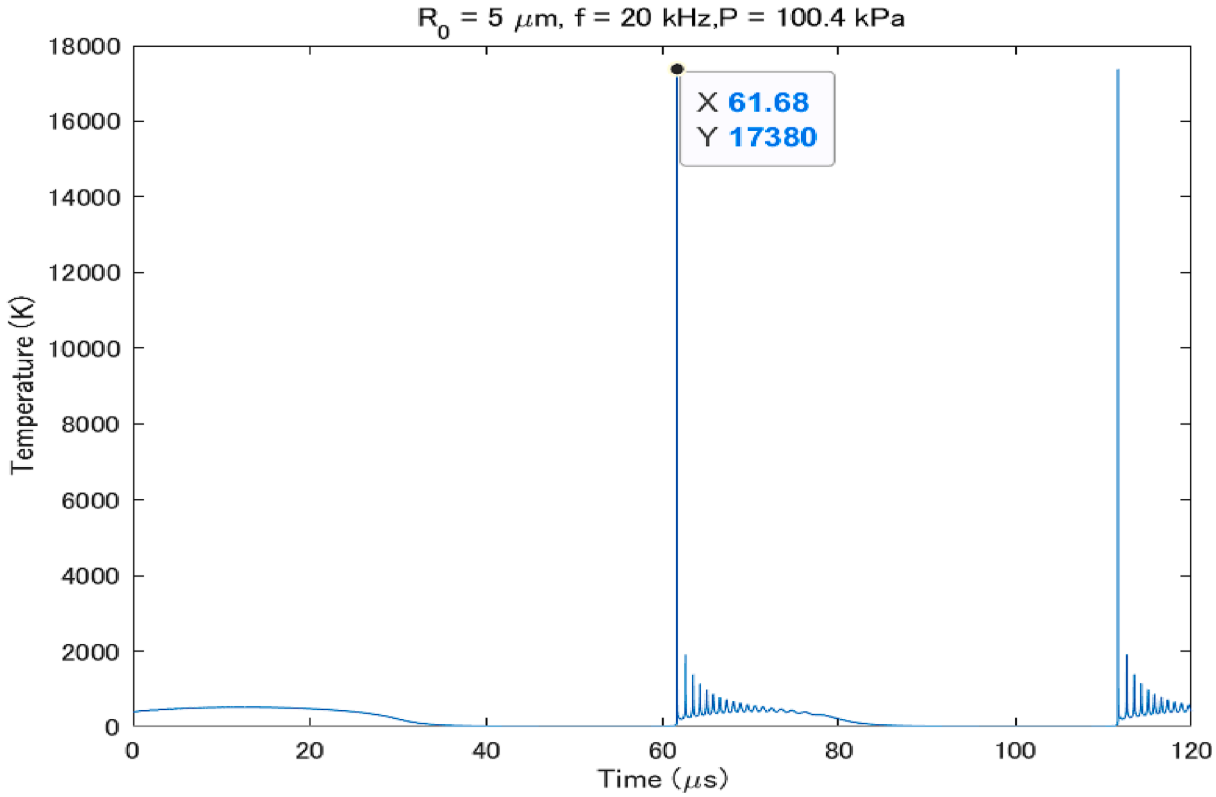

Fig. 16. Time variation of bubble temperature.

ultrasound irradiation was completed. Due to the promotion of nucleation by ultrasound irradiation, a significant portion of the solute in the product was used for nucleation. This could have resulted in a reduction of the solute used for particle growth, which may explain the limited growth of particles observed after 60 min of ultrasound irradiation.

4.5. *Effect of ultrasound irradiation on reaction rate*

Fig. 13 shows the relationship between reaction time and the unreacted percentage of terephthalic acid (α). The dotted line shows the value of α at the end of the reaction (after 24 h). The value of 0.063 at the end of the reaction indicates that a little terephthalic acid remains, but the value is very close to 0, which means that it is almost completely depleted. In the solvothermal method, terephthalic acid decreases slowly, and all terephthalic acid reacts after 24 h of reaction time. In the ultrasound-assisted synthesis method, the amount of terephthalic acid decreased rapidly upon ultrasound irradiation, and the reaction time of 120 min showed the same amount of terephthalic acid as at the end of the reaction. This is because ultrasound irradiation promoted nucleation and the synthesis of UiO-66, resulting in a rapid decrease in the amount of terephthalic acid, the raw material. Assuming that the time when the unreacted terephthalic acid ratio α takes the same value as the value after 24 h as the end of reaction, the reaction was completed in 300 min under the condition without ultrasound irradiation. Under the condition with ultrasound irradiation, the reaction time was reduced to less than half in 120 min. The reaction rate calculated from Fig. 13 without ultrasound irradiation was 4.43×10^{-3} min^{-1}, while that with ultrasound irradiation was 6.55×10^{-3} min^{-1}. Two factors are considered to be responsible for this difference in reaction rate. The first is the formation of hot spots due to cavitation [21]. In the reaction process of UiO-66, the solvent DMF thermally decomposes to dimethylamine at high temperature. Since the resulting dimethylamine is a strong base, the pH of the reaction solution increases, and deprotonation of the organic ligands occurs. The MOF structure is formed by the bonding of the deprotonated portion with metal ions. The second is the increase of collision between solute molecules. As shown in Eq. (10), Arrhenius equation predicts the rate of a chemical reaction at a given temperature and frequency factor A, which represents the frequency of collision between reacting

molecules, increases with ultrasound irradiation when the synthesis by ultrasound is compared with that by heating [22]. In addition, the bubbles created by cavitation are collapsed and generate flow in the reactor. The occurring flow facilitates mass transfer of the solute and increase the frequency of collisions. As a result, the reaction rate is considered to be increased.

4.6. Temperature at the collapse of cavitation bubble

To investigate the factors which promote nucleation, the temperature at the collapse of cavitation bubble due to ultrasound cavitation was calculated using MATLAB® (Math Works Co., Ltd.). The medium in the reactor was N,N-dimethylformamide (DMF), and the physical properties of DMF at 293 K were used. Fig. 14 shows the calculated results of the expansion rate of the bubbles over time. The bubbles showed a large expansion followed by contraction. This rapid contraction causes the bubble to collapse, resulting in a large amount of energy. Fig. 15 shows the results of the bubble wall velocity calculations. A large velocity is generated when the bubble is collapsed. This is due to the rapid contraction of the bubble, which causes the bubble to collapse and flow due to its inability to withstand the pressure from the outside. Fig. 16 shows the calculated temperature change over time in the bubbles. The temperature inside the bubble reached 17380 K during the rapid contraction of the bubble. The simulation confirmed the formation of hot spots and the flow during bubble collapse. In fact, the time scale of the very high temperature is very short relative to the time scale of the reaction and has little effect on the overall reaction. In nucleation, however, the time scale of this phenomenon is also very short, and the authors believe that the creation of a very momentary high temperature field could have an effect on nucleation.

5. Conclusion

This study investigated the effects of ultrasound irradiation on the particle size and reaction process of UiO-66 in the initial stage of synthesis.

First, study compared the particle size of UiO-66 synthesized by the solvothermal and ultrasound-assisted synthesis methods. The particles synthesized by the ultrasound-assisted synthesis method were smaller than those synthesized by the solvothermal method. This indicates that ultrasound irradiation contributes to the reduction of particle size. It was also found that the particle size did not change significantly when the ultrasound irradiation time was longer than 10 min.

A comparison of the cloudiness rate in the reactor shows that the ultrasound irradiation-assisted synthesis method generates nuclei more rapidly than the solvothermal method, and the induction time and transient period are reduced. This is thought to be due to the fact that ultrasound irradiation causes cavitation, which in turn promotes nucleation due to the high temperature conditions. The unreacted rate of terephthalic acid, the organic ligand of UiO-66, also suggests that nucleation is promoted. Numerical simulation revealed that the temperature inside the bubble is very high at ca. 17300 K.

These results suggest that ultrasound irradiation has an effect on promoting nucleation and reducing the particle size of UiO-66. In particular, UiO-66 with a very small particle size is obtained after 3 min of ultrasound irradiation.

This method, in which ultrasound is applied only in the initial stages of the reaction, has proven to be very effective in terms of process intensification.

CRediT authorship contribution statement

Yu Ogura: Data curation, Investigation, Writing – original draft. **Keita Taniya:** Conceptualization, Methodology. **Kuo-Lun Tung:** Methodology. **Satoru Nishiyama:** Methodology. **Yoshiyuki Komoda:** Methodology. **Naoto Ohmura:** Supervision, Funding acquisition, Writing – review & editing.

Declaration of Competing Interest

The authors declare that they have no known competing financial interests or personal relationships that could have appeared to influence the work reported in this paper.

Acknowledgment

This work was supported by JSPS KAKENHI Grant Numbers JP 18H03853, JP 19KK0127. The authors wish to thank Mr. Norihisa Kumagai for his experimental support.

References

[1] L.J. Murray, M. Dinca, J.R. Long, Hydrogen storage in metal–organic frameworks, Chem. Soc. Rev. 38 (2009) 1294–1314.
[2] X. Kang, G. Fu, Z. Song, G. Huo, F. Si, X. Deng, X.Z. Fu, J.L. Luo, Microwave-assisted hydrothermal synthesis of MOFs-derived bimetallic CuCo-N/C electrocatalyst for efficient oxygen reduction reaction, J. Alloy. Compd. 795 (2019) 462–470.
[3] D. Nagatomo, T. Horie, C. Hongo, N. Ohmura, Effect of ultrasonic pretreatment on emulsion polymerization of styrene, Ultrason. Sonochem. 31 (2016) 337–341.
[4] H.-Y. Kim, S.-N. Kim, J. Kim, W.-S. Ahn, Sonochemical Synthesis of UiO-66 for CO2 Adsorption and Xylene Isomer Separation, Korean Chem. Eng. Res. 51 (4) (2013) 470–475.
[5] V. Safarifard, A. Morsali, Applications of ultrasound to the synthesis of nanoscale metal–organic coordination polymers, Coord. Chem. Rev. 292 (2015) 1–14.
[6] Z.Q. Li, L.G. Qiu, T. Xu, Y. Wu, W. Wang, Z. Y. Wu, X. Jiang, Ultrasonic synthesis of the microporous metal–organic framework Cu3(BTC)2 at ambient temperature and pressure: An efficient and environmentally friendly method, Mater. Lett. 63 (2009) 78–8.
[7] L.-G. Qiu, Z.-Q. Li, Y. Wu, W. Wang, T. Xu, X. Jiang, Facile synthesis of nanocrystals of a microporous metal–organic framework by an ultrasonic method and selective sensing of organoamines, Chem. Commun. (31) (2008) 3642.
[8] M.R. Armstrong, S. Senthilnathan, C.J. Balzer, B. Shan, L. Chen, B. Mu, Particle size studies to reveal crystallization mechanisms of the metal organic framework HKUST-1 during sonochemical synthesis, Ultrason. Sonochem. 18 (2017) 365–370.
[9] S. Mei, H. Lin, N. L. Guang, Q. Y. Peng, Y. Xia, J, An. Jian, X. Y. H, S. J. Zhu, Facile synthesis of highly luminescent nanowires of a terbium-based metal–organic framework by an ultrasonic-assisted method and their application as a luminescent probe for selective sensing of organoamines, Inorg. Chem. Commun. 17 (2012) 147-150.
[10] J.H. Cavka, S. Jakobsen, U. Olsbye, N. Guillou, C. Lamberti, S. Bordiga, K. P. Lillerud, A new zirconium inorganic building brick forming metal organic frameworks with exceptional stability, J. Am. Chem. Soc. 130 (2008) 13850–13851.
[11] S.H. Jhung, J.H. Lee, J.-S. Chang, Crystal size control of transition metal ion-incorporated aluminophosphate molecular sieves: Effect of ramping rate in the syntheses, Micropor. Mesopor. Mater. 112 (1-3) (2008) 178–186.
[12] A. Schaate, P. Roy, A. Godt, J. Lippke, F. Waltz, M. Wiebcke, P. Behrens, Modulated Synthesis of Zr-Based Metal-Organic Frameworks: From Nano to Single Crystals, Chem. Eur. J. 17 (24) (2011) 6643–6651.
[13] Chemical Engineering Handbook, Society of Chemical Engineers Japan, Maruzen Publishing (1999) in Japanese.
[14] P. Attri, P. Madhusudan Reddy, P. Venkatesu, Density and ultrasonic sound speed measurements for N, N-dimethylformamide with ionic liquids, Indian J. Chem. 49A (2010) 736–742.
[15] W. Lauterborn, T. Kurz, R. Mettin, P. Koch, D. Koroninger, D. Schanz, Acoustic cavitation and bubble dynamics, Arch. Acoust. 33 (4) (2008) 609–617.
[16] A. Jmbrak, Z. Herceg, D. Šubaric, J. Babic, Mladen Brncic, S. Rimac, T. Bosiljkov, D. Čvek, B. Tripalo, J. Gelo, Ultrasound effect on physical properties of corn starch, Carbohydr. Polym. 79 (2010) 91–100.
[17] Y. Bai, Y. Dou, L. Xie, W. Rutledge, J. Li, H. Zhou, Zr-based metal–organic frameworks: design, synthesis, structure, and applications, Chem. Soc. Rev. 45 (2016) 2327–2367.
[18] L. Bahrig, S.G. Hickey, A. Eychmuller, Mesocrystalline materials and the involvement of oriented attachment – a review, Cryst. Eng. Comm. 16 (2014) 9408–9424.
[19] C. Fang, W. Tang, S. Wu, J. Wang, Z. Gao, J. Gong, Ultrasound-assisted intensified crystallization of L-glutamic acid: Crystal nucleation and polymorph transformation, Ultrason. Sonochem. 68 (2020) 105227.

[20] V. Salinas, Y. Vargas, O. Louisnard, L. Gaete, Influence of the liquid viscosity on the formation of bubble structures in a 20 kHz field, Ultrason. Sonochem. 22 (2015) 227–234.
[21] H. Naeimi, F. Kiani, Ultrasound-promoted one-pot three component synthesis of tetrazoles catalyzed by zinc sulfide nanoparticles as a recyclable heterogeneous catalyst, Ultrason. Sonochem. 27 (2015) 408–415.
[22] E. Haque, N. Khan, J. Park, S.H. Jhung, Synthesis of a metal–organic framework material, iron terephthalate, by ultrasound, microwave, and conventional electric heating: A kinetic study, Chem. Eur. J. 16 (3) (2010) 1046–1052.